INTERFACE

royalsocietypublishing.org/journal/rsif

Review

**Cite this article:** Tarbell J, Mahmoud M, Corti A, Cardoso L, Caro C. 2020 The role of oxygen transport in atherosclerosis and vascular disease. *J. R. Soc. Interface* **17**: 20190732. http://dx.doi.org/10.1098/rsif.2019.0732

Received: 24 October 2019
Accepted: 11 March 2020

**Subject Category:**
Life Sciences–Engineering interface

**Subject Areas:**
bioengineering, biomedical engineering, biomechanics

**Keywords:**
hypoxia, atherosclerosis, vascular stent, helical stent, vasa vasorum, oxygen transport

**Author for correspondence:**
John Tarbell
e-mail: jtarbell@ccny.cuny.edu

THE ROYAL SOCIETY PUBLISHING

# The role of oxygen transport in atherosclerosis and vascular disease

John Tarbell[1], Marwa Mahmoud[1], Andrea Corti[1], Luis Cardoso[1] and Colin Caro[2]

[1]Biomedical Engineering Department, The City College of New York, New York, NY, USA
[2]Department of Bioengineering, Imperial College London, London, UK

JT, 0000-0001-6696-0272; AC, 0000-0003-0774-4064; LC, 0000-0002-2252-7802

Atherosclerosis and vascular disease of larger arteries are often associated with hypoxia within the layers of the vascular wall. In this review, we begin with a brief overview of the molecular changes in vascular cells associated with hypoxia and then emphasize the transport mechanisms that bring oxygen to cells within the vascular wall. We focus on fluid mechanical factors that control oxygen transport from lumenal blood flow to the intima and inner media layers of the artery, and solid mechanical factors that influence oxygen transport to the adventitia and outer media via the wall's microvascular system—the vasa vasorum (VV). Many cardiovascular risk factors are associated with VV compression that reduces VV perfusion and oxygenation. Dysfunctional VV neovascularization in response to hypoxia contributes to plaque inflammation and growth. Disturbed blood flow in vascular bifurcations and curvatures leads to reduced oxygen transport from blood to the inner layers of the wall and contributes to the development of atherosclerotic plaques in these regions. Recent studies have shown that hypoxia-inducible factor-1α (HIF-1α), a critical transcription factor associated with hypoxia, is also activated in disturbed flow by a mechanism that is independent of hypoxia. A final section of the review emphasizes hypoxia in vascular stenting that is used to enlarge vessels occluded by plaques. Stenting can compress the VV leading to hypoxia and associated intimal hyperplasia. To enhance oxygen transport during stenting, new stent designs with helical centrelines have been developed to increase blood phase oxygen transport rates and reduce intimal hyperplasia. Further study of the mechanisms controlling hypoxia in the artery wall may contribute to the development of therapeutic strategies for vascular diseases.

## 1. Introduction and background

The hypoxia theory of atherosclerosis proposes that an imbalance between the demand for and supply of oxygen in the arterial wall is a key factor in the development of intimal hyperplasia and atherosclerotic plaques. Recent review papers [1–3] have described the biomolecular mechanisms that advance atherosclerotic plaques in the presence of hypoxia. There is substantial evidence that there are regions within the atherosclerotic plaque in which significant hypoxia exists that may change the function, metabolism and responses of many of the cell types found within the developing plaque, and dictate whether the plaque will evolve into a stable or unstable phenotype.

Hypoxia-inducible factor-1α (HIF-1α), is a transcription factor that orchestrates the hypoxic response in cells and has been regarded as the 'master regulator of hypoxia' (figure 1). Under normoxic conditions (physiological levels of oxygen—greater than about 5% or 40 mm Hg), HIF-1α becomes targeted for degradation through proline hydroxylation by HIF prolyl hydroxylase (PHD) which results in a conformational change promoting its binding to Von Hippel–Lindau disease tumour suppressor protein (VHL) E3 ligase complex, which in turn targets HIF-1α for ubiquitination and rapid

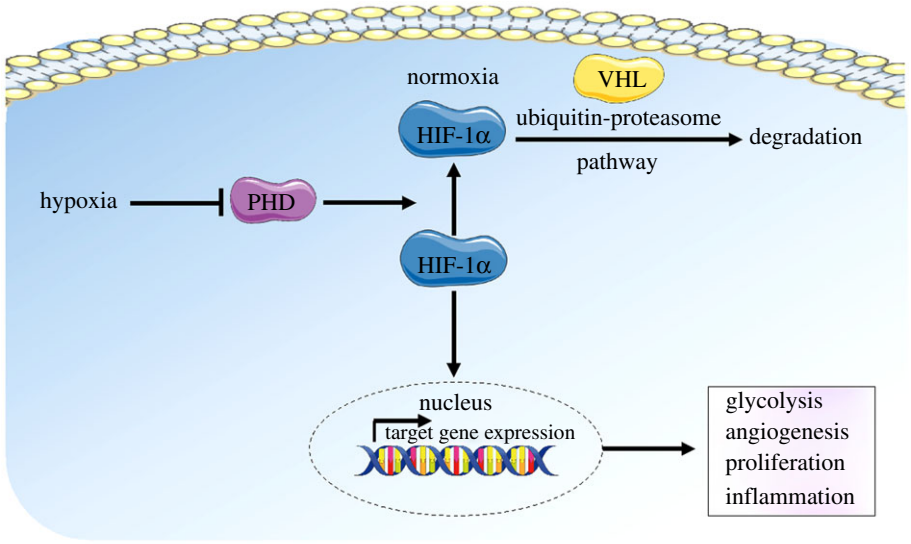


**Figure 1.** Schematic of hypoxic signalling. In normoxia, HIF-1α becomes targeted for degradation through proline hydroxylation by HIF prolyl hydroxylase (PHD). This results in a conformational change in HIF-1α, promoting its binding to VHL E3 ligase complex, and targeting HIF-1α for ubiquitination and rapid proteasomal degradation. In hypoxia, HIF-1α degradation is inhibited, resulting in its accumulation in the cells, and leading to its nuclear translocation and HIF1-α target gene expression. HIF-1α target genes mediate changes in cell function, including proliferation, angiogenesis, glycolysis and inflammation.

proteasomal degradation. In hypoxia, HIF-1α degradation is inhibited, resulting in its accumulation in the cells, leading to its nuclear translocation and HIF-1α target gene expression. HIF-1α target genes mediate inflammation, proliferation, angiogenesis and glycolysis [3].

Inflammatory disease states are often characterized as either being a result of tissue hypoxia or in activating hypoxia [4]. Thus, it is not surprising that hypoxia and inflammation share common signalling pathways; of major importance is NF-κB activation. It was first reported in 1994 by Koong *et al.* [5] that hypoxia activates NF-κB signalling by triggering the degradation of inhibitory IκB-a, resulting in the release of p65 (RelA) from the inhibitory complex and translocation into the nucleus where it promotes the transcription of NF-κB target genes. Since then, there have been numerous studies that demonstrate the activation of the inflammatory NF-κB pathway in hypoxia (reviewed in [4,6]). Consistent with this, it has also been shown that NF-κB signalling triggers HIF-1α activation in immune cells. In response to macrophage stimulation by bacterial infection, lipopolysaccharides (LPS) or hypoxia, active NF-κB signalling triggers the activation of HIF-1α [7,8]. In endothelial cells, non-canonical hypoxic signalling triggered by disturbed blood flow in the vasculature results in the activation of HIF-1α through NF-κB [9]. Interestingly, both NF-κB and HIF-1α can be activated by the same stimuli, this includes proinflammatory cytokines such as TNF-α and interleukin-6, oxidative stress and disturbed blood flow [8,9].

In concert with inflammation, hypoxia also triggers glucose metabolic changes in cells. Under low oxygen levels this change in metabolism is required to maintain adequate ATP production in cells [10]. Under inflammatory conditions, HIF-1α triggers the activation of glycolysis genes in endothelial cells [9]. In macrophages, the production of LPS by bacterial infection triggers glycolysis through HIF-1α [7].

In endothelial cells, the glycolysis shift caused by HIF-1α gives rise to enhanced cell proliferation and inflammation [9,11]. HIF-1α also triggers endothelial–mesenchymal transition [12,13], a process that results in further enhancement of inflammation, proliferation and permeability and has been shown to trigger atherosclerosis [14,15]. All of these changes in endothelial cell function are a hallmark of a dysfunctional endothelium which leads to the development of atherosclerosis.

While the biomolecular mechanisms relating hypoxia to atherosclerosis have been well described, the biophysical mechanisms responsible for hypoxia and its localization to regions of the vasculature where atherosclerosis develops have received less attention. Thus, a major aim of this review is to elucidate the biophysical mechanisms responsible for hypoxia, and to suggest methods to ameliorate hypoxia that derive from biophysical understanding.

We begin with a discussion of the pathways for oxygen transport to the arterial wall emphasizing transport to the inner layers from luminal blood flow and the outer layers from the supporting microvascular network—the vasa vasorum (VV). The role of VV compression leading to medial layer hypoxia in vascular disease is elucidated and the pathways for inflammatory response and plaque development provided by the VV are described. Impaired blood phase oxygen transport characteristics in regions of branching and curvature where atherosclerotic plaques localize are then discussed. It is well known that these are regions of disturbed flow that induce endothelial cell dysfunction, and recent studies show that even HIF-1α is upregulated by disturbed flow. But, here, it is emphasized that these are typically regions of vessel wall hypoxia as well. The final sections of the review deal with vascular stenting that reduces downstream hypoxia but can induce vessel wall hypoxia, intimal hyperplasia and restenosis within the stented region. The effects of stent expansion on VV compression and reduced blood flow to the outer layers of the wall are reviewed. A final section describes the biophysical effects of a stent with a helical centreline that promotes enhanced oxygen transport to the inner layers of the wall by virtue of the secondary flows induced by the helical geometry and reduces intimal hyperplasia.

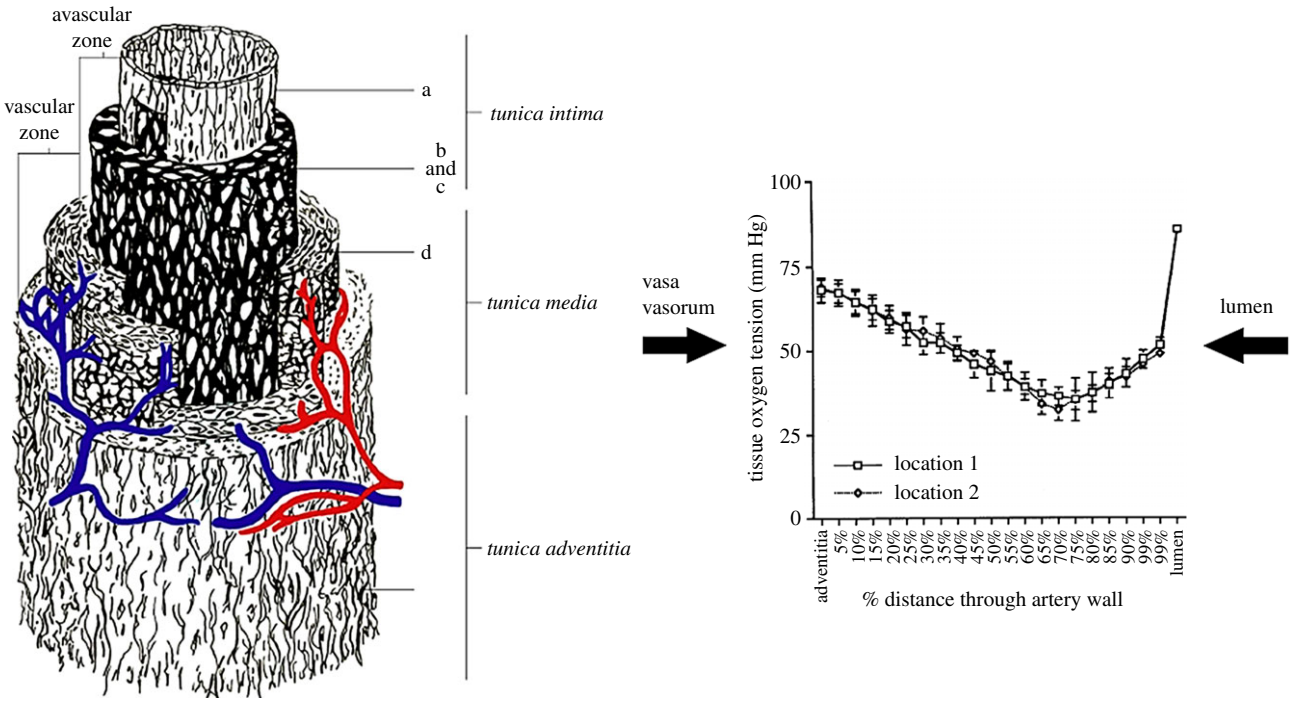


**Figure 2.** Two main pathways for oxygen transport to the blood vessel wall. (*a*) The intima and inner media are supplied from the luminal blood whereas the adventitia and outer media are supplied by the vasa vasorum [16]. (*b*) Arterial wall oxygen tension profile in the common carotid artery of a dog [17].

## 2. Pathways for oxygen transport to the arterial wall

There are two principal pathways for oxygen transport to the arterial wall: the inner layers (intima and inner media) receive oxygen primarily from lumenal blood flow and the outer layers (adventitia and outer media) from the VV, a microvascular network whose principal function is to service the outer regions of thicker blood vessels (figure 2*a*).

Depending on their origin, VV are divided into three categories [18]: vasa vasorum interna (VVI), when the origin is the main lumen itself and the branching network remains inside the arterial wall; vasa vasorum externa (VVE), when the origin is located outside the vascular wall and comes from a major branch emerging from the main lumen; venous vasa vasorum (VVV), when the tree structure starts from a neighbouring vein. The pattern of VV penetration into the outer layers of the wall is dependent on the wall thickness. Wolinsky & Glagov [19] examined thoracic aortic segments of 12 mammalian species and observed that mammals whose aortas had 29 or fewer medial lamellar units had no demonstrable intramural vascular channels (penetrating VV); those whose aortas had more than 29 medial lamellar units, had medial VV [19]. Aortas with medial VV always had a subintimal medial zone devoid of VV. Remarkably, the thickness of the avascular zone was about 0.47 mm in all species, suggesting that diffusive transport from the inner most VV and the lumen is limited to this distance. Williams *et al*. [20] pointed out that in normal arteries, VV from the adventitia grow into the media of large arteries and veins and actively regulate blood flow to the wall of these vessels [20]. But in atherosclerotic arteries, VV proliferate into the intima-media, where they provide nutrition to the thickened artery. These neovascular channels are thin-walled, however, and may contribute to intraplaque haemorrhage, plaque disruption and mural thrombosis. Choi *et al*. [21] identified macrophages and microchannels in mild coronary atherosclerosis supporting the role of inflammation and VV proliferation in the early stage of coronary atherosclerosis.

Niinikoski *et al*. [22] demonstrated that a transarterial wall oxygen gradient is present in normal rabbit aortas with oxygen tensions falling from the adventitia, reaching a nadir at the junction of the inner one-third and outer two-thirds of the vessel wall. This was demonstrated more clearly with oxygen microelectrode measurements by Santilli *et al*. [17]. A typical oxygen tension profile across a healthy artery (in this case, the common carotid artery of a dog) is displayed in figure 2*b*. Oxygen tension drops precipitously from the lumen to the inner most regions of the wall, suggesting a significant oxygen transport resistance in the near wall region of the lumen. This is followed by a more gradual drop in oxygen tension in the inner layers as oxygen supplied from the lumen is consumed by the cells in the media (primarily smooth muscle cells in the undiseased artery). The oxygen tension also drops gradually in the outer layers as fibroblasts and smooth muscle cells consume oxygen. The steadily falling oxygen tensions away from the adventitial surface suggest that the carotid artery wall is not supplied by any penetrating vessels from the VV. This is expected because the reported thickness of the vessel segment (0.204 mm) is well below the expected avascular zone thickness (0.47 mm) reported by Wolinsky & Glagov [19]. This was supported by light-microscopic examination which revealed VV only on the adventitial surface.

## 3. The role of oxygen transport pathways in vascular disease

### 3.1. Transport from the vasa vasorum

Early studies in the aortic media of dogs [23] indicated that VV provide a considerable amount of blood flow to the

outer wall layers of the thoracic aorta. The vessels were responsive to physiologic stimuli as they dilated during infusion of adenosine and constricted during acute hypertension. They speculated that reduction of blood flow to the aortic wall via the VV in hypertension might contribute to aortic medial necrosis.

More recent studies in humans showed that aortic dissections initially developed in the outer third of the media, alongside VV, which showed sclerotic changes. It was suggested that dysfunction of VV in hypertension may play a key role in ischaemia and associated malnutrition of the aortic media leading to the initiation of dissection [24]. These observations are consistent with the earlier review of Baikoussis *et al*. [25].

Booth *et al*. [26] developed a model of atherosclerosis by positioning a hollow silastic collar around the carotid artery of cholesterol-fed rabbits resulting in macrophage and smooth muscle cell infiltration into the arterial subendothelium, foam cell formation and deposition of extracellular lipid, all in the presence of a morphologically intact endothelium. They proposed that the changes induced by the collar were mediated by obstruction of the adventitial VV and the creation of localized wall hypoxia. This concept of VV occlusion leading to outer wall ischaemia and progression to atherosclerosis was further elaborated by Martin *et al*. [27].

Analytical and numerical modelling of the deformation of venous and arterial VV were developed by Maurice *et al*. [28]. A nonlinear elastic vessel wall model showed that a normal range of intraluminal pressure induces a small deformation in the VV in arteries but a larger deformation in VVV. Increased luminal pressure was predicted to compress VV and reduce flow, thereby resulting in reduced oxygen transport to the outer wall. More recently, Ritman & Lerman [18] stressed that acute modulation of VV patency due to surrounding compressive forces within the vessel wall and due to variable tone in the smooth muscle affect the progression of atherosclerotic plaques.

Compressive stress (tone) in the arterial media that may induce VV deformation and wall hypoxia has been assessed indirectly through pulse wave velocity (PWV) measurements relying on the classical Moens–Korteweg formula that relates PWV to the elastic modulus (Young's modulus $E$) of the wall as described in the below equation, where $h$ is the wall thickness, $r$ is the artery radius and $\rho$ is the density

$$\mathrm{PWV} = \sqrt{\frac{E \cdot h}{2r\rho}}. \tag{3.1}$$

Caro *et al*. [29], by means of non-invasive multichannel Doppler ultrasound measurements of PWV, showed that cigarette smoking in healthy subjects increases arterial wall stiffness ($E$). In a related study, Tarnawski *et al*. [30] observed increased PWV in subjects with a nicotine patch. Levenson *et al*. [31] found that PWV was increased significantly in hypertensive subjects compared to normotensive controls. Tarnawski *et al*. [32] determined significantly higher PWV in non-athletes compared to age-matched athletes. Psychosocial stress/anxiety have also been shown to increase PWV [33]. All of these factors that increase PWV are considered risk factors for cardiovascular disease. Szmigielski *et al*. [34] showed that PWV correlates with aortic atherosclerosis as characterized by intimal–medial thickness. The implication of these studies is that increased vessel wall compression associated with elevated PWV (E) compresses VV leading to outer wall hypoxia and vascular dysfunction.

But the link between increased wall stiffness (PWV) and hypoxia does not appear to have been demonstrated directly. There is, however, indirect evidence for such a link. First, PWV as an indicator of arterial stiffness has been validated clinically in large arteries [35]. In addition, with increased pressure in the aorta and increased rigidity in the arterial wall associated with systemic arterial hypertension, VV blood flow decreases, presumably a result of VV compression [18,36] and this results in local hypoxia and aortic medial necrosis. In support of this view, experimental ligation of the VV results in medial aortic necrosis in dogs [37].

## 3.2. The vasa vasorum in atherosclerotic plaque development

The initiation and progression of atheromas [38–40] is characterized by elevated plasma lipid concentration (hypercholesterolaemia) [41] and increased transport of low-density lipoprotein (LDL) across an impaired endothelium [42,43]. Dysfunctional endothelium develops under the influence of hypertension, free radicals and inappropriate flow shear stress. Contrary to the long-standing belief that the vast majority of LDL transport occurs at the luminal side of the vessel, recent studies have shown that adventitial VV play a significant role in the initiation and/or progression of vascular disease [44,45]. Endothelial dysfunction in both the arterial lumen and the arterial VV leads to delivery of LDL, oxidized and inflammatory products, at a rate [46] greater than the clearance by VVV [47]. Phagocytes are attracted into the vessel wall, and a chronic vascular inflammatory environment (i.e. increased expression of NF-κB) initiates the process of local plaque formation [48]. Another consequence of infiltration of lipids, accumulation of macrophages, release of cytokines and angiogenic stimulus generated by oxidative stresses in the vessel wall is the proliferation of VV [49–53]. Accumulation of inflammatory cells in the intima stimulates the proliferation of smooth muscle cells in the media, and as a consequence, the vessel wall undergoes positive remodelling, increasing its wall thickness.

Thickening of the vessel wall changes the transmural pressure gradient and wall tissue stresses, and creates regions with low oxygen tension in the medial layer [54,55], where metabolic needs exceed the amount of oxygen that can diffuse from the lumen [56,57]. The blood flow resistance is high in the distal VV located close to the media layer. High wall tissue stresses within the intima and medial layers of the wall can exceed the blood pressure in VV at that location, and significantly restrict blood flow through them. Also, VV blood flow may be selectively reduced by increased smooth muscle tone in proximal VV due to inflammation or thrombosis. These mechanisms can result in insufficient removal of waste products and local hypoxia in the media layer.

Reduced perfusion from VV promotes increased progression of fatty streaks, further increasing oxygen demand [58] in the intima layer, resulting in local hypoxia. Thus, higher VV density is required to meet the oxygen perfusion needs of the arterial wall. Hypoxia triggers local VV neovascularization via the production of angiogenic factors. Studies in hypertensive rats demonstrated increase in HIF-1α and

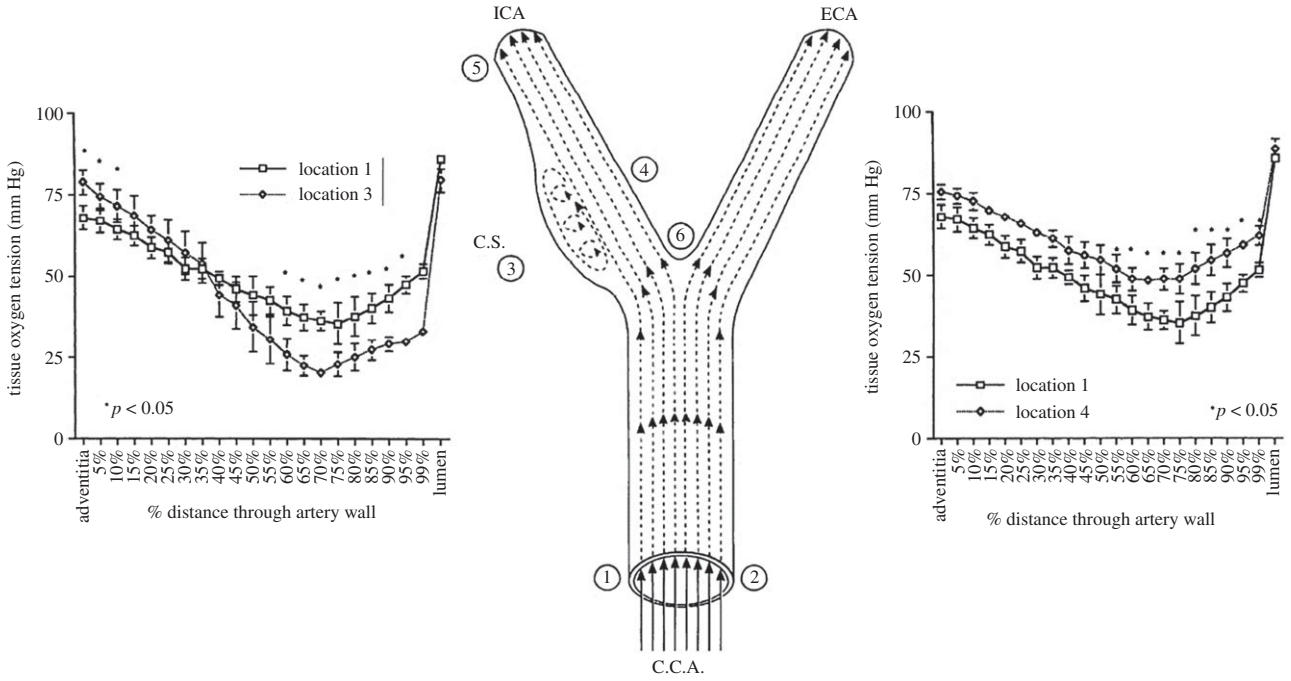


**Figure 3.** Intra-arterial oxygen tension profiles in dog carotid artery. (Left) Comparison of profiles in the common carotid (position 1) and the disturbed flow carotid sinus (position 3). (Right) Comparison of profiles in the common carotid (position 1) and the stable flow inner wall (position 4). From Santilli *et al*. [17].

angiogenic factors [49,51–53], including VEGF expression in the aorta, which was subsequently followed by increase in VV density around the aorta [59]. A similar increase in HIF-1α and VEGF has been demonstrated in coronary arteries in hypercholesterolaemic pigs [60]. The reversibility of endothelial dysfunction at the early stages of atherosclerosis is associated with a reduction in VV density (neovascularization). Moreover, anti-angiogenic therapy reduced plaque neovascularization and plaque growth [61], and it was associated with a reduction of macrophages in the plaque and around the VV [20,62].

Neovascularization within atherosclerotic plaques leads to VV that are immature. These vessels lack a smooth muscle cell layer, tight junctions and a continuous basement membrane [63]. Dysfunctional VV lead to stasis of blood flow, loss of endothelial barrier function, increased vascular permeability and extravasation of fluids and proteins [64,65]. Unfortunately, proliferation of ruptured and/or leaky VV seems to facilitate the ingress of pro-atherogenic cellular and soluble plasma components, including macrophages and inflammatory factors into the vessel wall, thus further enhancing angiogenesis [62] and the progression of atherosclerosis [66]. Leaky VV within the atheroma core lead to intraplaque haemorrhage [63,67,68]. Extravasated erythrocytes come in contact with plaque lipid, and undergo haemolysis followed by oxidation of haemoglobin and release of free haem or iron, which accumulates within the plaque [69]. Also, haemoglobin/haem released from phagocytosed erythrocytes by macrophages contributes to the iron deposition in lesions [70], necrotic core size and increased macrophage density [71]. VV haemorrhage is a key factor in the development of unstable atherosclerotic lesions [71,72]. VV is twofold denser in vulnerable plaques and fourfold denser in ruptured plaques, when compared with stable plaques [73,74].

In summary, initiation and progression of VV neovascularization in atherosclerosis is driven by both chronic inflammatory and hypoxic environments within the tissue [75,76]. Angiogenesis of VV is a physiological response of the organism to restore the appropriate nutrition and oxygen supply in the vessel wall; however, dysfunctional VV neovascularization (i.e. increased intraplaque VV density with impaired endothelium) further contributes to plaque inflammation [77], intraplaque haemorrhage [71], thin-cap fibroatheromas [68] and acute cardiovascular events [63,68].

## 3.3. Transport from the lumen

Experiments in dogs [17] (figure 3) show significant induction of inner wall hypoxia in the disturbed flow region of the internal carotid artery (carotid sinus—region 3) compared to the common carotid artery (region 1), and reduction of inner wall hypoxia in the stable flow region of the internal carotid (region 4). The minimum $PO_2$ in region 3 is about 21 mm Hg, region 1 is 38 mm Hg and region 4 is 46 mm Hg. It has been shown that there is a steep rise (fourfold) in HIF-1α concentration in human umbilical vein endothelial cells (HUVECs) as $PO_2$ levels drop from 38 mm Hg (5%) to 23 mm Hg (3%) [78]. In a recent review paper, 3% oxygen (23 mm Hg) has been described as moderate hypoxia, whereas 5% (38 mm Hg) is considered borderline hypoxic [2]). Thus, it appears that the $PO_2$ of 21 mm Hg in the carotid sinus represents a hypoxic state relative to the inner wall (46 mm Hg) and the common carotid (38 mm Hg).

The hypoxic region in the carotid sinus (region 3 in figure 3) has been shown to be a region of low fluid wall shear stress (WSS) compared to the common carotid artery, whereas region 4 is characterized by higher shear stress [79,80]. These observations suggest that fluid phase transport of oxygen to the blood vessel wall is controlling oxygen tension in the inner wall region. This hypothesis is suggested by the Leveque theory of mass transport in thin boundary layers [81], indicating that the rate of fluid phase oxygen transport to the wall, as characterized by the mass transport coefficient

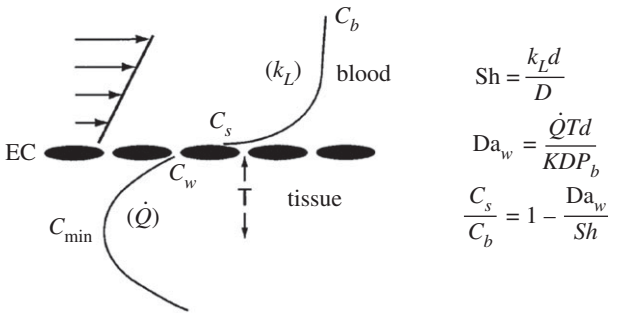


**Figure 4.** Outline of simplified mass transport considerations for oxygen transport to a blood vessel wall. The schematic displays the concentration profile from the bulk blood ($C_b$) to the endothelial cell surface ($C_s$) to the inner wall ($C_w$) and the minimum value ($C_{min}$) as indicated in figure 2. $k_L$ is the fluid phase mass transport coefficient, $\dot{Q}$ is the oxygen consumption rate and $T$ is the distance to $C_{min}$—roughly ½ the wall thickness. The velocity profile at the left is linearized because of the thin concentration boundary layer (Leveque approximation) [81].

$k_L$ (figure 4), is proportional to the wall shear rate (WSS/viscosity) to the 1/3 power. And, it is well known that region 3 develops atherosclerotic plaques, whereas regions 1 and 4 are typically spared [82–84].

The theory of fluid phase transport to an artery wall has been elaborated in several studies, many in the context of LDL transport. See, for example, representative cases of 'wall free models' [85], 'single layer models' [86] and 'multilayer models' [87]. These studies have also examined the importance of non-Newtonian blood flow modelling on transport and found non-Newtonian effects to be of minor importance. For models of oxygen transport, the early paper of Crawford *et al.* [88], followed by the study of Moore & Ethier [89] and more recently Murphy *et al.* [90] are representative of developments in oxygen transport modelling. Tarbell [91] presented a simplified single layer model that is summarized in figure 4. By assuming that endothelial cells offer no transport resistance for highly diffusible oxygen ($C_w = C_s$) and that oxygen consumption by smooth muscle cells in the wall is the limiting rate process within the wall (oxygen diffusion is rapid), a simple expression for the surface concentration relative to the bulk concentration is obtained

$$\frac{C_s}{C_b} = 1 - \frac{\mathrm{Da}_w}{\mathrm{Sh}}. \tag{3.2}$$

In the above equation, the Damhkoler number ($Da_w$) is the dimensionless wall oxygen consumption rate and the Sherwood number (Sh) is the dimensionless fluid phase mass transfer coefficient. The Sh or dimensionless mass transfer coefficient ($Sh = k_L d/D$) introduces the fluid phase mass transfer coefficient ($k_L$), vessel lumen diameter ($d$) and oxygen diffusion coefficient in the tissue ($D$). The Damkholer number ($Da_w = \dot{Q}Td/KDP_b$) is the dimensionless oxygen consumption rate ($\dot{Q}$) within the wall: $T$ is the half-thickness of the wall and $P_b$ is the bulk oxygen tension (related to $C_b$ through the Henry's law relationship $C = KP$, where $K$ is the Henry's law constant).

For a fixed oxygen consumption rate (fixed $Da_w$), when the fluid phase mass transfer rate is large ($Sh \gg Da_w$) then $C_s \rightarrow C_b$ and there is no limitation from fluid phase mass transport (the wall consumption is limiting). However, for lower rates of fluid phase transport, $Sh \rightarrow Da_w$, and $C_s \rightarrow 0$ (the blood phase mass transport is limiting). Note that equation (3.1) predicts negative surface concentrations when $Sh < Da_w$. This derives from an assumption in the analysis that $PO_2$ in the tissue is well above the value of the Michaelis constant in a Michaelis–Menten description of the kinetics of oxygen consumption. The Michaelis constant is typically of order 1 mm Hg [92] and $PO_2$ in the deep wall is well above that level (figure 2). Values for $Da_w$ based on data in the literature for oxygen consumption in arteries range between 11 and 49 [91].

Subsequent detailed computer simulations of oxygen transport in the carotid bifurcation, neglecting oxygen binding to haemoglobin [93], revealed more clearly the fluid phase transport limitations in the carotid sinus (figure 5). The colour-coded concentration profiles show a uniform $PO_2$ entry profile at 90 mm Hg. The wall boundary condition was taken to be zero, consistent with an assumption of fluid phase transport limitation. The cross-sectional oxygen concentration distributions are shown in the four panels at the top of the figure. There is a clear prediction of reduced fluid phase oxygen concentration in the carotid sinus region that is consistent with the observations in figure 3. The Sh calculations show regions of highly reduced Sh in the carotid sinus along with regions of elevated Sh on the opposite wall—again quite consistent with the data in figure 2. Note also that regions of low Sh co-localize with regions of low WSS, although there is not a complete overlap of the two regions (figure 5 right). Moore & Ethier [89] had pointed out inaccuracies associated with the neglect of haemoglobin binding, but they do not alter the basic conclusions of Tada & Tarbell [93].

Related computer simulations for a curved artery approximating the curvature of a coronary artery over the surface of the heart have been described [94]. For typical coronary artery curvatures, flow conditions and transport properties characteristic of oxygen, the results indicate a large difference in Sh between the outside (Sh about 55) and inside (Sh about 2) walls, implying that $O_2$ transport at the inner wall could be limited by the fluid phase. More generally, the inner curvature of arteries is also a region of relatively low WSS [9] and a site for localization of atherosclerosis [95].

## 4. Disturbed flow activates HIF-1α

Although HIF-1α activation by hypoxia is the canonical pathway, interestingly a number of recent studies revealed that HIF-1α can be activated non-canonically, through mechanical activation. Wu *et al.* [11] show that disturbed blood flow (which exerts a low, oscillating shear stress on the surface of endothelial cells lining arteries) in porcine arteries led to elevated levels of HIF-1α. Consistent with this, Feng *et al.* [9] show that HIF-1α was also elevated at sites of disturbed flow in porcine and murine arteries. A study by Fernandez Esmerats *et al.* [96] shows that HIF-1α was enhanced in endothelial cells exposed to disturbed flow located at the fibrosa

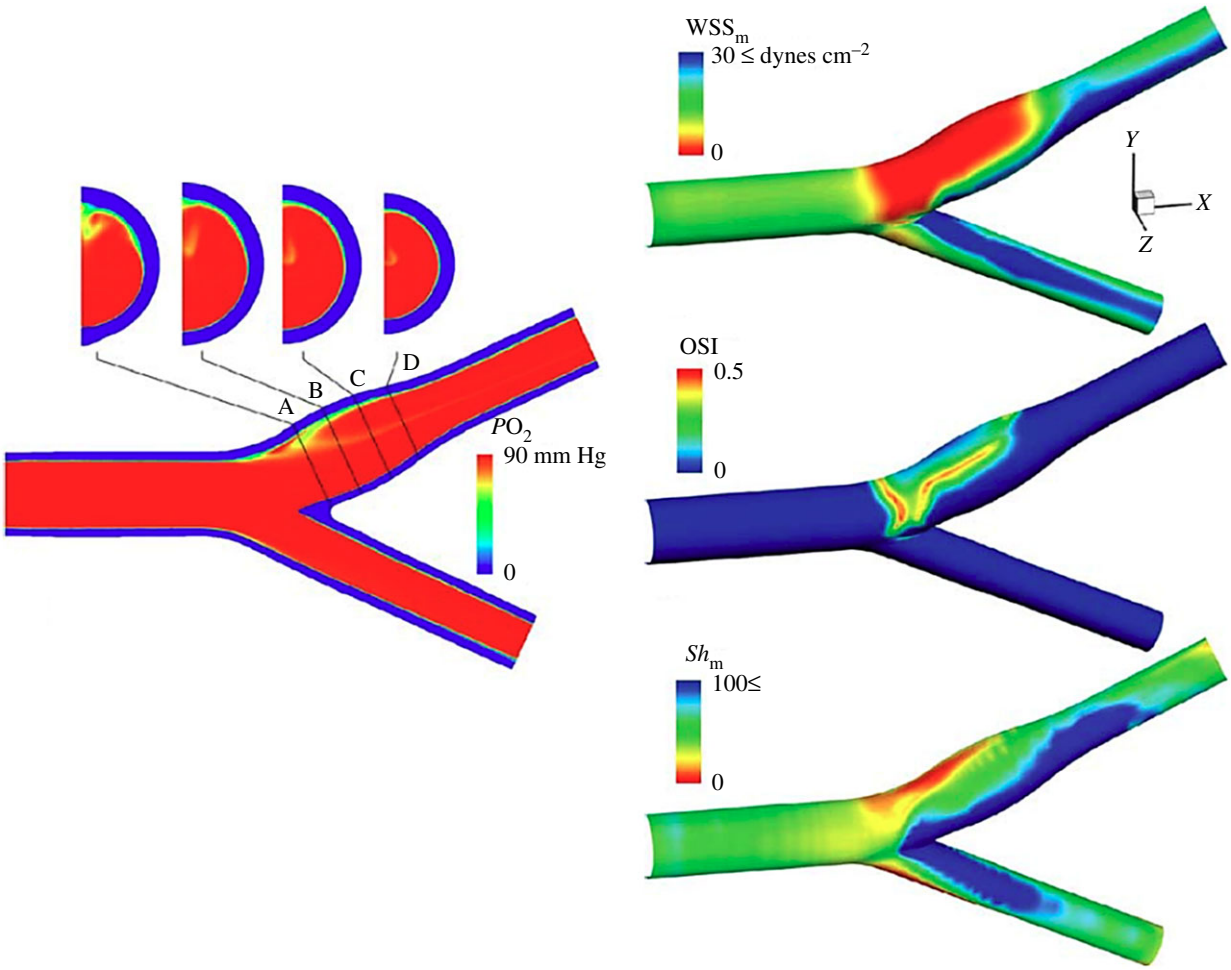


**Figure 5.** Computer simulations of fluid phase oxygen transport in the carotid bifurcation. Colour coding on the left panels indicates $PO_2$ levels. Note in the right panel that red is indicative of low Sh and blue of high Sh. Based on Tada & Tarbell [93].

side of the aortic valve of human patients. These studies revealed that HIF-1α can be activated by disturbed blood flow *in vivo*. In addition, these studies, using *in vitro* flow systems that recapitulate the shear stress *in vivo*, show that endothelial cells exposed to disturbed flow under normoxic conditions had elevated HIF-1α mRNA and protein levels [9,11,96]. Thus, it appears from these findings that both hypoxia induced by disturbed flow, and disturbed flow itself can induce HIF-1α expression.

The activation of HIF-1α by disturbed flow is linked to the induction of endothelial cell dysfunction and subsequent atherogenesis and calcific aortic valve disease. In response to disturbed flow, HIF-1α has been shown to be activated through NFκB proinflammatory signalling, along with stabilization by the debiquitinating enzyme cezanne [9]. Elevated HIF-1α levels in turn trigger the activation of glycolysis genes, leading to a metabolic reprogramming of cells and elevated levels of inflammation and proliferation, and these in turn are hallmarks of a dysfunctional endothelium which promotes atherogenesis [9,11]. Wu *et al.* [11] suggest that the mechanism by which disturbed flow activates HIF-1α is through reactive oxygen species (ROS) generating oxidase NOX4, which leads to elevated HIF-1α levels and downstream activation of proinflammatory NFκB signalling, enhanced glycolysis and endothelial cell dysfunction. Interestingly, HIF-1α activation by disturbed flow can be controlled epigenetically. Fernandez Esmerats *et al.* show that downregulation of miR483 by disturbed flow leads to elevated HIF-1α levels in endothelial cells through enhanced expression of a miR483-target gene UBE2C, which functions as an ubiquitinating protein that degrades VHL, leading to HIF-1α accumulation. Elevated HIF-1α levels promote inflammation and endothelial–mesenchymal transition in endothelial cells, leading to dysfunction and calcification in the aortic valve [96].

Non-canonical activation of HIF-1α by disturbed flow appears to play an important role in the progression of disease. However, it also appears that these pro-atherogenic disturbed flow areas are hypoxic, and that disturbed flow along with hypoxia play a dual role in switching on HIF-1α-mediated endothelial cell dysfunction leading to disease progression in arteries.

## 4.1. Atherosclerosis is not common in veins

If hypoxia plays a role in atherosclerosis, and $PO_2$ is much lower in venous blood than arterial blood, why is atherosclerosis not common in veins? While this question appears not to have been answered conclusively in the literature, several contributing mechanisms have been described. Even though the $PO_2$ of venous blood (about 40 mm Hg) is much lower than arterial blood (about 100 mm Hg), vein wall oxygenation is achieved by diffusion of oxygen from blood in the lumen as well as the VV, much like arteries [97]. The VV of saphenous veins and tributaries, for example, originate from feeding arteries in the surrounding adipose tissue and

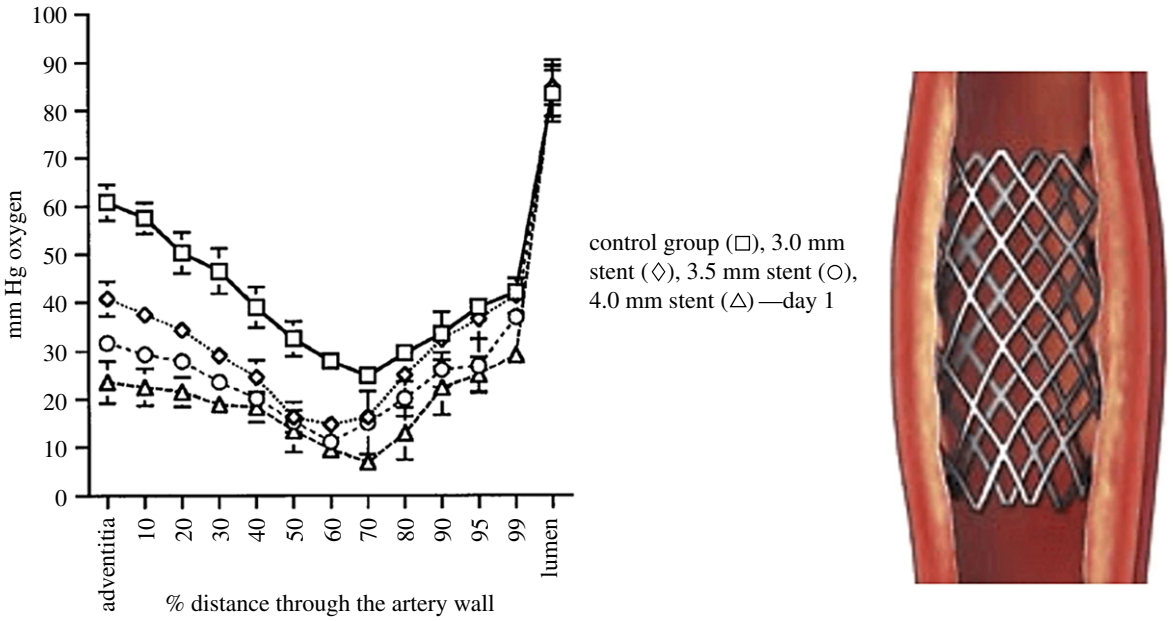


**Figure 6.** Stent expansion induces outer wall hypoxia. Oxygen tension data at various stent expansions in the distal aorta of rabbits at 1 day after stenting [106].

penetrate into the media and adventitia of the vein wall providing arterial levels of oxygen to the outer wall regions. Thus, the outer layers of veins may experience arterial oxygen levels. It has been suggested that defects in this mechanism lead to vein wall hypoxia that is a contributing factor for varicose vein formation [98]. Varicose veins are characterized by intimal hyperplasia and smooth muscle cell dysfunction without the lipid accumulation associated with atherosclerotic plaques in arteries [99].

In the venous system of the lower limbs, a series of bicuspid valves ensure blood flow movement in the cephalad direction, preventing the reflux of blood towards the feet while in the upright posture. The venous valves are characterized by flow separation from their leaflets leading to disturbed flow that tends to be atherogenic in arteries (recall figure 3). Disturbed flow may lead to clotting and deep vein thrombosis but not lipid deposition and atherosclerosis [100].

Veins are generally protected from lipid deposition. In an early work, McCluskey & Wilens [101] observed no trace of lipid in the intima or media of any sections prepared from veins removed from 20 patients. A plausible mechanism for this observation was presented later by Lever & Jay [102]. They determined that the medial layer of the inferior vena cava was about one-third the thickness of the media in the carotid artery of rabbits. In addition, the porosity of the medial layer of the vena cava to macromolecules was about 10 times that of the carotid artery. They suggested that the thin medial layer with high porosity in veins compared to arteries may permit easy drainage of macromolecules (LDL) preventing their accumulation in the wall, thereby contributing to the low susceptibility of these vessels to atherosclerotic disease.

## 5. Stent hypoxia

The most reliable treatment for symptomatic vascular narrowing is percutaneous transluminal angioplasty (PTA), which widens the narrowed sections of the artery using a catheter balloon and often placing a medical stent, a slender, expandable, cylindrical metal mesh in the region of vascular occlusion [103]. The stent works as a mechanical support for the vascular wall, re-opening the pathological region and restoring the original blood flow. However, PTA with stenting is often complicated by in-stent restenosis secondary to neointimal hyperplasia, which may result in failure of the implant. Although restenosis is linked to different aspects of the procedure, recent studies have highlighted the relationship between reduced levels of oxygen tension within the stented artery wall and intimal hyperplasia [90,104–107]. The stent itself plays a key role in determining the overall oxygen supply to the underlying tissue. Even though the stent restores the required blood flow to downstream vasculature, it may induce a hypoxic condition for the arterial layers around the stent.

It is widely believed that intimal hyperplasia following stenting is the result of an inflammatory response to intimal damage during stent implantation and expansion [108,109] as well as a material reaction in the case of polymer-coated stents [110]. The initial IH response occurs rapidly (within one week) and may become significant at one to three months. In addition, decreased oxygen tensions have been noted throughout the artery wall immediately following stent deployment with a return towards control values at 28 days in a rabbit model (figure 6). Larger stent deployment diameters yielded acutely lower artery wall oxygen tensions.

Inner wall hypoxia during stenting appears to be driven by increased smooth muscle cell oxygen consumption associated with cellular compression during the acute phase of response (days) after stent deployment [106]. This increased demand for oxygen can lead to a supply limitation from the blood phase as discussed in the context of figure 2. In addition, inner wall hypoxia may be associated with reduced fluid phase transport driven by local flow separation around stent struts [90,111]. The endothelial layer is also damaged during stenting [112], but the endothelium itself offers very little resistance to oxygen transport and is not expected to be influential in controlling wall hypoxia [91].

Outer wall hypoxia appears to be driven by reduced oxygen transport through the VV. It has been suggested, but not observed directly, that VV deformation associated

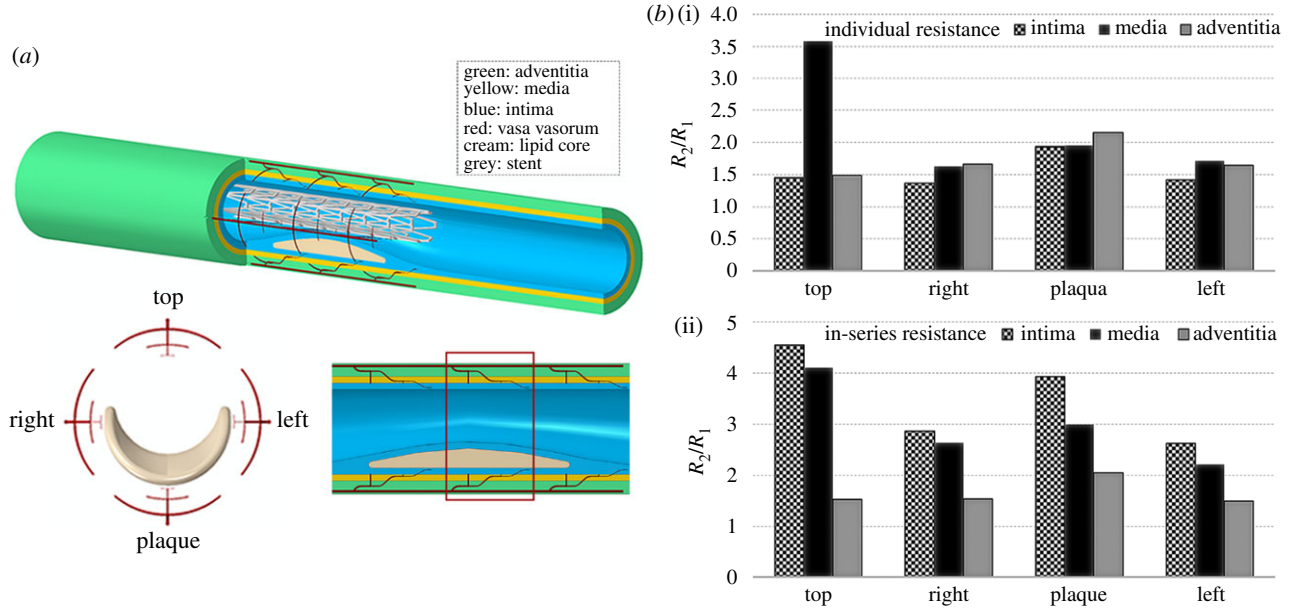


**Figure 7.** (*a*) Illustration of the plaque, VV, stent model in lateral section. (*b*) Fold increase in resistance to flow (pressure drop/flow) for over-expanded stent (1.3 : 1). Histograms report both the individual change in resistance at each layer (i) and the resulting augmentation due to the vessels in-series layout (ii). Results refer to VV in the central region in the red rectangle (*a*) [121].

with increased wall compression in stenting is responsible for outer wall hypoxia. This mechanism would be exaggerated in stent overexpansion as possibly reflected in Santilli *et al*. [106] showing greater outer wall hypoxia with stent overexpansion (figure 6).

Cheema *et al*. [105] showed that outer wall hypoxia after stenting leads to upregulation of VEGF and PDGF inducing an angiogenic response that ultimately increases outer wall microvessel density over a period of four weeks. This may in part account for the observed reduction in outer wall hypoxia after four weeks of stenting observed by Santilli *et al*. [106]. However, this mechanism provides a new pathway for inflammatory response, macrophage infiltration and associated wall thickening that may exacerbate intimal hyperplasia as discussed in the earlier section on VV in atherosclerotic plaque development.

Consistent with evidence for wall hypoxia after stenting is the recent report of Li *et al*. [113] who showed that hyperbaric oxygen therapy after coronary stenting improved patients' myocardial circulation compared to a control group with stents but without oxygen therapy. Earlier work in rabbits had shown that supplemental oxygen reduces IH after stent deployment [107]. Additional work in rabbits indicated that supplemental oxygen inhibits IH and SMC proliferation after creation of an arterio-venous fistula and prolongs patency [114].

## 5.1. Deformation of vasa vasorum after stenting

Previous research has focused its attention on understanding the effect of disruption of blood flow through VV [115–117]. The results are often medial necrosis, stagnant interstitial fluid, decreased vascular wall nutrition and wall hypoxia. All of these may occur when the artery is stent-expanded. Stent-expanded arteries may reach sufficiently elevated degrees of deformation such that high circumferential and radial stresses could compress VV, thus diminishing blood flow through VV and reducing oxygen delivery to the outer layers of the vessel wall. During stent expansion, circumferential stresses in the layers remain rather small as long as the elastic fibres are able to stretch. Once they reach the maximum extension, the stress begins to increase exponentially as collagen, which is 100–1000 times stiffer than elastin, bears increasing load [106]. On the other hand, radial stress is the compressive component responsible for squeezing the structures in the artery wall. Increments in both circumferential and radial stresses likely affect the original VV morphology, and may contribute to artery wall hypoxia. This mechanism naturally implies a relation between final stent diameter, arterial stress and VV diameter that could provide the link between transarterial wall oxygen gradient and the degree of stent expansion [106,117]. In clinical practice, stents are routinely expanded under fluoroscopy to achieve a stent/artery luminal diameter ratio of 1.1 : 1. However, it can happen that the implant exceeds this limit, reaching a situation of overexpansion where the ratio is 1.2 : 1 or greater. Stent expansion may compress the VV, resulting in reduction of vascular wall blood perfusion leading to wall hypoxia. Previous studies have used finite-element analysis (FEA) to investigate the mechanical interaction between expanded stents and atherosclerotic tissues [118–120]. Others have focused on the influence of the implant design on the haemodynamics and oxygen transport rates through the stented lumen [90,117].

A very recent study implemented FEA to explore VV compression induced by stenting, assessing whether the final stent diameter could induce a hypoxic situation in the outer vascular layers [121]. An idealized multi-layered fibroatheroma model was created (figure 7*a*) comprising the intima, media and adventitia layers as thick-walled nonlinear elastic cylindrical tubes. The plaque was modelled as a semi-annular lipid core placed in the intimal layer, causing a 60% stenosis. Four VV trees were oriented symmetrically around the vessel (figure 7*a*) with three branches of decreasing diameter in the axial and radial direction, penetrating into each vascular layer. The stent was expanded to reach a stent/


**Figure 8.** The helical stent reduces intimal hyperplasia. (*a*) Image of a helical stent; (*b*) reduction of intimal hyperplasia 30 days after helical stent implantation in pig common carotid arteries [104].

artery lumen diameter ratio of 1.1 : 1, 1.2 : 1 and 1.3 : 1 in different simulations. The results indicated large increases in resistance to blood flow (pressure drop/flow) with stent expansion. Assuming the pressure drop between the VV inlet and outlet remain constant, the blood flow would drop more than four times in the media and intima when considering the in-series network organization of longitudinal, descending branches (figure 7*b*). These increases in hydraulic resistance could potentially lead to a hypoxic condition, especially when the stent is over-expanded.

### 5.2. Altered stent geometry enhances fluid phase mass transport

In addition to anti-proliferative [122] and anti-inflammatory [123] drug release from stents to suppress IH, and hyperbaric oxygen to directly ameliorate the effects of hypoxia on IH after stenting [113], an approach based on alteration of blood flow mechanics and blood phase oxygen transport rates was introduced by Shinke *et al*. [124] and described in greater detail by Caro's group [104,125,126]. They modified a commercially available bare-metal, nitinol, self-expanding stent by introducing a helical-centreline geometry (figure 8*a*). The helical geometry induces secondary flows (in the plane perpendicular to the axial flow) that alter fluid shear stress and mass transport characteristics. The new stent design was initially tested in straight sections of pig common carotid arteries with a conventional straight centreline stent in one CCA and the helical stent in the contralateral CCA. After 30 days, there was a 45% reduction in intimal thickness associated with the helical stent compared to the straight stent (figure 8*b*). In addition, there was a 40% reduction in the number of adventitial microvessels associated with the helical stent, suggesting a reduction in wall hypoxia. A subsequent human clinical trial of patients with peripheral artery disease showed improved patency of the superficial femoral artery out to two years when treated with a helical stent compared to a straight stent [127]. All of this is consistent with recent studies from De Nisco *et al*. [128] suggesting the atheroprotective nature of helical flow in the coronary arteries.

Computer simulations of flow in the helical stent versus the straight stent [125,126] showed that the helical stent enhances WSS and mass transfer rate (indicated by the Sh) significantly—about threefold for both WSS and Sh. In addition, it was shown that shear stress gradients in the peripheral direction are induced by secondary flow in the helical stent, whereas there are no peripheral gradients for straight stents. Increased WSS has been shown to suppress IH [129,130]. It has been demonstrated that increased nitric oxide production, a normal response of endothelial cells to increased WSS, suppresses smooth muscle cell proliferation, reducing oxygen consumption and migration from media to intima [131]. These mechanisms contribute to reduced IH in high WSS. The possible effects of shear stress gradients, independent of shear stress magnitude, on stent performance are not known. Although wall oxygen tensions were not measured, it is expected that elevated mass transfer rates (Sh) reduce wall hypoxia (recall figure 4). Estimation of the level of reduction through modelling has not been attempted, but would require measurements of smooth muscle and fibroblast oxygen consumption rates beneath an expanded stent as critical input information. Then the simple model described in figure 4 or more sophisticated models could be examined to estimate oxygen tensions within the wall.

## 6. Summary

1. Hypoxia in the vascular wall leads to the upregulation of the transcription factor HIF-1α that induces pro-atherogenic genes enhancing cell proliferation, inflammation and angiogenesis.
2. Oxygen is transported to the intima and inner media from luminal blood flow and to the adventitia and outer media by VV blood flow.
3. Elevated compressive stresses in the outer layers of the wall associated with hypertension, smoking and other cardiovascular risk factors reduce blood flow by compressing the VV.
4. Adventitial VV play a significant role in the initiation and progression of vascular disease.
5. Dysfunctional VV neovascularization contributes to plaque inflammation, intraplaque haemorrhage, thin-cap fibroatheromas and acute cardiovascular events.
6. Disturbed blood flow in vascular bifurcations and curvatures leads to reduced oxygen transport from blood to the inner layers of the wall. These regions of disturbed

flow are associated with the development of atherosclerotic plaques.

7. HIF-1α is also activated in disturbed flow by a mechanism that is independent of hypoxia.
8. Both hypoxia and disturbed flow in regions of vessel bifurcation and curvature conspire to upregulate HIF-1α that induces vascular dysfunction and atherogenesis.
9. Vascular stenting to open a diseased blood vessel induces both outer and inner wall hypoxia which are exaggerated by stent overexpansion. This hypoxia leads to neointimal hyperplasia that may evolve to restenosis.
10. Inner wall hypoxia is primarily driven by the increased oxygen consumption of compressed cells (smooth muscle and fibroblasts), although disturbed flow around stent struts may reduce oxygen transport from the lumen in the early response (until the struts are covered by neo-intima). Outer wall hypoxia is secondary to VV compression reducing blood flow to the outer layers in addition to cell compression.
11. Stent overexpansion exacerbates hypoxia by increasing wall stresses and VV compression.
12. To overcome oxygen transport limitations from lumenal blood flow, helical stents have been developed that induce secondary flows to enhance oxygen transport rates. Early animal and human studies of the helical stent show reduced intimal hyperplasia compared to straight stents.

Data accessibility. This article does not contain any additional data.

Authors' contributions. J.T. conceived the scope of the review, coordinated the review, organized the manuscript; M.M. contributed to several sections; A.C. contributed to sections and manuscript design; L.C. contributed to several sections; C.C. conceived the scope of the review and contributed to several sections. All authors gave final approval for publication and agree to be held accountable for the work performed therein.

Competing interests. We declare we have no competing interests.

Funding. J.T. was supported by NIH grant nos. RO1CA204949, F32HL145913 (M.M.); L.C. was supported by NIH grant nos. R01HL136431, SC1DK103362 and NSF grant no. CMMI-1662970; C.C. was supported by Garfield Weston Foundation.

## References

1. Marsch E, Sluimer JC, Daemen MJ. 2013 Hypoxia in atherosclerosis and inflammation. *Curr. Opin. Lipidol,* **24**, 393–400. (doi:10.1097/MOL.0b013e32836484a4)
2. Ferns GAA, Heikal L. 2017 Hypoxia in atherogenesis. *Angiology* **68**, 472–493. (doi:10.1177/0003319716662423)
3. Semenza GL. 2012 Hypoxia-inducible factors in physiology and medicine. *Cell* **148**, 399–408. (doi:10.1016/j.cell.2012.01.021)
4. Bartels K, Grenz A, Eltzschig HK. 2013 Hypoxia and inflammation are two sides of the same coin. *Proc. Natl Acad. Sci. USA* **110**, 18 351–18 352. (doi:10.1073/pnas.1318345110)
5. Koong AC, Chen EY, Giaccia AJ. 1994 Hypoxia causes the activation of nuclear factor κ B through the phosphorylation of I κ B α on tyrosine residues. *Cancer Res.* **54**, 1425–1430.
6. D'Ignazio L, Rocha S. 2016 Hypoxia induced NF-kappaB. *Cells* **5**, 10.
7. Tannahill GM *et al.* 2013 Succinate is an inflammatory signal that induces IL-1β through HIF-1α. *Nature* **496**, 238–242. (doi:10.1038/nature11986)
8. D'Ignazio L, Bandarra D, Rocha S. 2016 NF-κB and HIF crosstalk in immune responses. *FEBS J.* **283**, 413–424. (doi:10.1111/febs.13578)
9. Feng S *et al.* 2017 Mechanical activation of hypoxia-inducible factor 1α drives endothelial dysfunction at atheroprone sites. *Arter. Thromb. Vasc. Biol.* **37**, 2087–2101. (doi:10.1161/ATVBAHA.117.309249)
10. Corcoran SE, O'Neill LAJ. 2016 HIF1α and metabolic reprogramming in inflammation. *J. Clin. Invest.* **126**, 3699–3707. (doi:10.1172/JCI84431)
11. Wu D *et al.* 2017 HIF-1α is required for disturbed flow-induced metabolic reprogramming in human and porcine vascular endothelium. *eLife* **6**, e25217. (doi:10.7554/elife.25217.044)
12. Xu X, Tan X, Tampe B, Sanchez E, Zeisberg M, Zeisberg EM. 2015 Snail is a direct target of hypoxia-inducible factor 1alpha (HIF1α) in hypoxia-induced endothelial to mesenchymal transition of human coronary endothelial cells. *J. Biol. Chem.* **290**, 16 653–16 664. (doi:10.1074/jbc.M115.636944)
13. Zhang B, Niu W, Dong HY, Liu ML, Luo Y, Li ZC. 2018 Hypoxia induces endothelial–mesenchymal transition in pulmonary vascular remodeling. *Int. J. Mol. Med.* **42**, 270–278. (doi:10.3892/ijmm.2018.3584)
14. Mahmoud MM *et al.* 2016 TWIST1 integrates endothelial responses to flow in vascular dysfunction and atherosclerosis. *Circ. Res.* **119**, 450–462. (doi:10.1161/CIRCRESAHA.116.308870)
15. Chen P-Y, Qin L, Baeyens N, Li G, Afolabi T, Budatha M, Tellides G, Schwartz MA, Simons M. 2015 Endothelial-to-mesenchymal transition drives atherosclerosis progression. *J. Clin. Invest.* **125**, 4514–4528. (doi:10.1172/JCI82719)
16. Herbst M, Holzenbein TJ, Minnich B. 2014 Characterization of the vasa vasorum in the human great saphenous vein: a scanning electron microscopy and 3D-morphometry study using vascular corrosion casts. *Microsc. Microanal.* **20**, 1120–1133. (doi:10.1017/S1431927614001287)
17. Santilli SM, Stevens RB, Anderson JG, Payne WD, Caldwell MD. 1995 Transarterial wall oxygen gradients at the dog carotid bifurcation. *Am. J. Physiol.* **268**, H155–H161.
18. Ritman EL, Lerman A. 2007 The dynamic vasa vasorum. *Cardiovasc. Res.* **75**, 649–658. (doi:10.1016/j.cardiores.2007.06.020)
19. Wolinsky H, Glagov S. 1967 Nature of species differences in the medial distribution of aortic vasa vasorum in mammals. *Circ. Res.* **20**, 409–421. (doi:10.1161/01.RES.20.4.409)
20. Williams JK, Armstrong ML, Heistad DD. 1988 Vasa vasorum in atherosclerotic coronary arteries: responses to vasoactive stimuli and regression of atherosclerosis. *Circ. Res.* **62**, 515–523. (doi:10.1161/01.RES.62.3.515)
21. Choi BJ, Matsuo Y, Aoki T, Kwon T-G, Prasad A, Gulati R, Lennon RJ, Lerman LO, Lerman A. 2014 Coronary endothelial dysfunction is associated with inflammation and vasa vasorum proliferation in patients with early atherosclerosis. *Arterioscler. Thromb. Vasc. Biol.* **34**, 2473–2477. (doi:10.1161/ATVBAHA.114.304445)
22. Niinikoski J, Heughan C, Hunt TK. 1973 Oxygen tensions in the aortic wall of normal rabbits. *Atherosclerosis* **17**, 353–359. (doi:10.1016/0021-9150(73)90026-9)
23. Heistad DD, Marcus ML, Law EG, Armstrong ML, Ehrhardt JC, Abboud FM. 1978 Regulation of blood flow to the aortic media in dogs. *J. Clin. Invest.* **62**, 133–140. (doi:10.1172/JCI109097)
24. Osada H, Kyogoku M, Ishidou M, Morishima M, Nakajima H. 2012 Aortic dissection in the outer third of the media: what is the role of the vasa vasorum in the triggering process? *Eur. J. Cardiothorac. Surg.* **43**, e82–e88. (doi:10.1093/ejcts/ezs640)
25. Baikoussis NG *et al.* 2011 The implication of vasa vasorum in surgical diseases of the aorta. *Eur. J. Cardiothorac. Surg.* **40**, 412–417.
26. Booth RF, Martin JF, Honey AC, Hassall DG, Beesley JE, Moncada S. 1989 Rapid development of atherosclerotic lesions in the rabbit carotid artery induced by perivascular manipulation. *Atherosclerosis* **76**, 257–268. (doi:10.1016/0021-9150(89)90109-3)
27. Martin JF, Booth RF, Moncada S. 1991 Arterial wall hypoxia following thrombosis of the vasa vasorum is an initial lesion in atherosclerosis. *Eur. J. Clin.*

*Invest.* **21**, 355–359. (doi:10.1111/j.1365-2362.1991.tb01382.x)
28. Maurice G, Wang X, Stoltz JF. 1998 Linear and nonlinear elastic modelling of the deformation of vasa vasorum. *Clin. Hemorheol. Microcirc.* **19**, 291–298.
29. Caro CG, Parker KH, Lever MJ, Fish PJ. 1987 Effect of cigarette smoking on the pattern of arterial blood flow: possible insight into mechanisms underlying the development of arteriosclerosis. *Lancet* **2**, 11–13. (doi:10.1016/S0140-6736(87)93052-2)
30. Tarnawski M, McLean M, Caro CG, Doorly DJ, Dumoulin CL. 1998 Effect of nicotine transdermal patch on femoral artery wavespeed in healthy human subjects measured by MRI. *J. Physiol.* **506P**, 16P.
31. Levenson J, Simon SC, Bouthier JD, Benetos A, Safar ME 1984 Post synaptic alpha blockade and brachial artery compliance in essential hypertension. *J. Hypertension* **2**, 37–41. (doi:10.1097/00004872-198402000-00007)
32. Tarnawski M, Cybulski G, Doorly D, Dumoulin C, Darrow R, Caro C. 1994 Noninvasive determination of local wavespeed and distensibility of the femoral artery by comb-excited Fourier velocity-encoded magnetic resonance imaging: measurements on athletic and nonathletic human subjects. *Heart Vessels* **9**, 194–201. (doi:10.1007/BF01746064)
33. Logan JG, Barksdale DJ, Carlson J, Carlson BW, Rowsey PJ. 2012 Psychological stress and arterial stiffness in Korean Americans. *J. Psychosom. Res.* **73**, 53–58. (doi:10.1016/j.jpsychores.2012.04.008)
34. Szmigielski C, Styczyński G, Sobczyńska M, Milewska A, Placha G, Kuch-Wocial A. 2016 Pulse wave velocity correlates with aortic atherosclerosis assessed with transesophageal echocardiography. *J. Hum. Hypertens.* **30**, 90–94. (doi:10.1038/jhh.2015.35)
35. Et-Taouil K, Safar M, Plante GE. 2003 Mechanisms and consequences of large artery rigidity. *Can. J. Physiol. Pharmacol.* **81**, 205–211. (doi:10.1139/y03-022)
36. Kohnken R, Scansen BA, Premanandan C. 2016 Vasa vasorum arteriopathy: relationship with systemic arterial hypertension and other vascular lesions in cats. *Vet. Pathol.* **54**, 475–483. (doi:10.1177/0300985816685137)
37. Marcus ML, Heistad DD, Armstrong ML, Abboud FM. 1985 Effects of chronic hypertension on vasa vasorum in the thoracic aorta. *Cardiovasc. Res.* **19**, 777–781. (doi:10.1093/cvr/19.12.777)
38. Fuster V, Fuster V, Badimon L, Badimon JJ, Chesebro JH. 1992 The pathogenesis of coronary artery disease and the acute coronary syndromes (2). *N Engl. J. Med.* **326**, 310–318. (doi:10.1056/NEJM199201303260506)
39. Fuster V, Fuster V, Badimon L, Badimon JJ, Chesebro JH. 1992 The pathogenesis of coronary artery disease and the acute coronary syndromes (1). *N Engl. J. Med.* **326**, 242–250. (doi:10.1056/NEJM199201233260406)
40. Busse R, Fleming I. 1996 Endothelial dysfunction in atherosclerosis. *J. Vasc. Res.* **33**, 181–194. (doi:10.1159/000159147)
41. Steinberg D. 1983 Lipoproteins and atherosclerosis. A look back and a look ahead. *Arteriosclerosis* **3**, 283–301. (doi:10.1161/01.ATV.3.4.283)
42. Lin SJ, Jan KM, Weinbaum S, Chien S. 1989 Transendothelial transport of low density lipoprotein in association with cell mitosis in rat aorta. *Arteriosclerosis* **9**, 230–236. (doi:10.1161/01.ATV.9.2.230)
43. Yin Y, Lim KH, Weinbaum S, Chien S, Rumschitzki DS. 1997 A model for the initiation and growth of extracellular lipid liposomes in arterial intima. *Am. J. Physiol.* **272**, H1033–H1046. (doi:10.1152/ajpheart.1997.272.2.h1033)
44. Wilcox JN, Scott NA. 1996 Potential role of the adventitia in arteritis and atherosclerosis. *Int. J. Cardiol.* **54**, S21–S35. (doi:10.1016/S0167-5273(96)02811-2)
45. Barker SG, Beesley JE, Baskerville PA, Martin JF. 1995 The influence of the adventitia on the presence of smooth muscle cells and macrophages in the arterial intima. *Eur. J. Vasc. Endovasc. Surg.* **9**, 222–227. (doi:10.1016/S1078-5884(05)80094-2)
46. Adams CW, Bayliss OB. 1969 The relationship between diffuse intimal thickening, medial enzyme failure and intimal lipid deposition in various human arteries. *J. Atheroscler. Res.* **10**, 327–339. (doi:10.1016/S0368-1319(69)80036-0)
47. Herrmann J, Lerman LO, Rodriguez-Porcel M, Holmes Jr DR, Richardson DM, Ritman EL, Lerman A. 2001 Coronary vasa vasorum neovascularization precedes epicardial endothelial dysfunction in experimental hypercholesterolemia. *Cardiovasc. Res.* **51**, 762–766. (doi:10.1016/S0008-6363(01)00347-9)
48. Wilson SH, Caplice NM, Simari RD, Holmes DR, Carlson PJ, Lerman A. 2000 Activated nuclear factor-kappaB is present in the coronary vasculature in experimental hypercholesterolemia. *Atherosclerosis* **148**, 23–30. (doi:10.1016/S0021-9150(99)00211-7)
49. Nordestgaard BG, Hjelms E, Stender S, Kjeldsen K. 1990 Different efflux pathways for high and low density lipoproteins from porcine aortic intima. *Arteriosclerosis* **10**, 477–485. (doi:10.1161/01.ATV.10.3.477)
50. Tufro-McReddie A, Norwood VF, Aylor KW, Botkin SJ, Carey RM, Gomez RA. 1997 Oxygen regulates vascular endothelial growth factor-mediated vasculogenesis and tubulogenesis. *Dev. Biol.* **183**, 139–149. (doi:10.1006/dbio.1997.8513)
51. SoRelle R. 1998 Two sides of the same coin: stop angiogenesis for cancer and encourage it for coronary artery disease. *Circulation* **98**, 383–384. (doi:10.1161/01.CIR.98.5.383)
52. Roberts WG, Palade GE. 1995 Increased microvascular permeability and endothelial fenestration induced by vascular endothelial growth factor. *J. Cell Sci.* **108**, 2369–2379.
53. D'Amato RJ, Loughnan MS, Flynn E, Folkman J. 1994 Thalidomide is an inhibitor of angiogenesis. *Proc. Natl Acad. Sci. USA* **91**, 4082–4085. (doi:10.1073/pnas.91.9.4082)
54. de Muinck ED, Simons M. 2004 Re-evaluating therapeutic neovascularization. *J. Mol. Cell. Cardiol.* **36**, 25–32. (doi:10.1016/j.yjmcc.2003.10.002)
55. Nagy JA, Dvorak AM, Dvorak HF. 2003 VEGF-A(164/165) and PlGF: roles in angiogenesis and arteriogenesis. *Trends Cardiovasc. Med.* **13**, 169–175. (doi:10.1016/S1050-1738(03)00056-2)
56. Heistad DD, Marcus ML, Larsen GE, Armstrong ML. 1981 Role of vasa vasorum in nourishment of the aortic wall. *Am. J. Physiol.* **240**, H781–H787. (doi:10.1152/ajpheart.1981.240.5.h781)
57. Heistad DD, Marcus ML. 1979 Role of vasa vasorum in nourishment of the aorta. *Blood Vessels* **16**, 225–238. (doi:10.1159/000158209)
58. Morrison AD, Clements RS, Winegrad AI. 1972 Effects of elevated glucose concentrations on the metabolism of the aortic wall. *J. Clin. Invest.* **51**, 3114–3123. (doi:10.1172/JCI107138)
59. Kuwahara F, Kai H, Tokuda K, Shibata R, Kusaba K, Tahara N, Niiyama H, Nagata T, Imaizumi T. 2002 Hypoxia-inducible factor-1α/vascular endothelial growth factor pathway for adventitial vasa vasorum formation in hypertensive rat aorta. *Hypertension* **39**, 46–50. (doi:10.1161/hy1201.097200)
60. Wilson SH, Herrmann J, Lerman LO, Holmes DR, Napoli C, Ritman EL, Lerman A. 2002 Simvastatin preserves the structure of coronary adventitial vasa vasorum in experimental hypercholesterolemia independent of lipid lowering. *Circulation* **105**, 415–418. (doi:10.1161/hc0402.104119)
61. Moulton KS, Heller E, Konerding MA, Flynn E, Palinski W, Folkman J. 1999 Angiogenesis inhibitors endostatin or TNP-470 reduce intimal neovascularization and plaque growth in apolipoprotein E-deficient mice. *Circulation* **99**, 1726–1732. (doi:10.1161/01.CIR.99.13.1726)
62. Moulton KS *et al.* 2003 Inhibition of plaque neovascularization reduces macrophage accumulation and progression of advanced atherosclerosis. *Proc. Natl Acad. Sci. USA* **100**, 4736–4741. (doi:10.1073/pnas.0730843100)
63. Virmani R, Kolodgie FD, Burke AP, Finn AV, Gold HK, Tulenko TN, Wrenn SP, Narula J. 2005 Atherosclerotic plaque progression and vulnerability to rupture: angiogenesis as a source of intraplaque hemorrhage. *Arterioscler. Thromb. Vasc. Biol.* **25**, 2054–2061. (doi:10.1161/01.ATV.0000178991.71605.18)
64. Bates DO, Hillman NJ, Williams B, Neal CR, Pocock TM. 2002 Regulation of microvascular permeability by vascular endothelial growth factors. *J. Anat.* **200**, 581–597. (doi:10.1046/j.1469-7580.2002.00066.x)
65. Langheinrich AC, Kampschulte M, Buch T, Bohle R, 2007 Vasa vasorum and atherosclerosis—quid novi? *Thromb. Haemost.* **97**, 873–879. (doi:10.1160/TH06-12-0742)
66. Nielsen LB. 1999 Atherogenecity of lipoprotein(a) and oxidized low density lipoprotein: insight from *in vivo* studies of arterial wall influx, degradation and efflux. *Atherosclerosis* **143**, 229–243. (doi:10.1016/S0021-9150(99)00064-7)
67. de Nooijer R, Verkleij CJ, von der Thusen JH, Jukema JW, van der Wall EE, van Berkel TJ, Baker AH, Biessen EA. 2006 Lesional overexpression of matrix metalloproteinase-9 promotes intraplaque hemorrhage in advanced lesions but not at earlier stages of

atherogenesis. *Arterioscler. Thromb. Vasc. Biol.* **26**, 340–346. (doi:10.1161/01.atv.0000197795.56960.64)

68. Moreno PR, Purushothaman KR, Fuster V, Echeverri D, Truszczynska H, Sharma SK, Badimon JJ, O'Connor WN. 2004 Plaque neovascularization is increased in ruptured atherosclerotic lesions of human aorta: implications for plaque vulnerability. *Circulation* **110**, 2032–2038. (doi:10.1161/01.CIR.0000143233.87854.23)
69. Yuan XM, Li W, Olsson AG, Brunk UT. 1996 Iron in human atheroma and LDL oxidation by macrophages following erythrophagocytosis. *Atherosclerosis* **124**, 61–73. (doi:10.1016/0021-9150(96)05817-0)
70. Lee TS, Pang JH, Chau LY. 1999 Erythrophagocytosis and iron deposition in atherosclerotic lesions. *Chin. J. Physiol.* **42**, 17–23.
71. Kolodgie FD *et al.* 2003 Intraplaque hemorrhage and progression of coronary atheroma. *N Engl. J. Med.* **349**, 2316–2325. (doi:10.1056/NEJMoa035655)
72. O'Brien KD, Mcdonald TO, Chait A, Allen MD, Alpers CE. 1996 Neovascular expression of E-selectin, intercellular adhesion molecule-1, and vascular cell adhesion molecule-1 in human atherosclerosis and their relation to intimal leukocyte content. *Circulation* **93**, 672–682. (doi:10.1161/01.CIR.93.4.672)
73. Kolodgie FD, Virmani R, Burke AP, Farb A, Weber DK, Kutys R, Finn AV, Gold HK. 2004 Pathologic assessment of the vulnerable human coronary plaque. *Heart* **90**, 1385–1391. (doi:10.1136/hrt.2004.041798)
74. Virmani R, Kolodgie FD, Burke AP, Farb A, Schwartz SM. 2000 Lessons from sudden coronary death: a comprehensive morphological classification scheme for atherosclerotic lesions. *Arterioscler. Thromb. Vasc. Biol.* **20**, 1262–1275. (doi:10.1161/01.ATV.20.5.1262)
75. Xu J, Lu X, Shi GP. 2015 Vasa vasorum in atherosclerosis and clinical significance. *Int. J. Mol. Sci.* **16**, 11 574–11 608. (doi:10.3390/ijms160511574)
76. Sedding DG, Boyle EC, Demandt JAF, Sluimer JC, Dutzmann J, Haverich A, Bauersachs J. 2018 Vasa vasorum angiogenesis: key player in the initiation and progression of atherosclerosis and potential target for the treatment of cardiovascular disease. *Front. Immunol.* **9**, 706. (doi:10.3389/fimmu.2018.00706)
77. Langheinrich AC, Michniewicz A, Sedding DG, Walker G, Beighley PE, Rau WS, Bohle RM, Ritman EL. 2006 Correlation of vasa vasorum neovascularization and plaque progression in aortas of apolipoprotein $E^{-/-}$/low-density lipoprotein$^{-/-}$ double knockout mice. *Arterioscler. Thromb. Vasc. Biol.* **26**, 347–352. (doi:10.1161/01.ATV.0000196565.38679.6d)
78. Keeley TP, Siow RCM, Jacob R, Mann GE. 2017 A PP2A-mediated feedback mechanism controls $Ca^{2+}$-dependent NO synthesis under physiological oxygen. *FASEB J.* **31**, 5172–5183. (doi:10.1096/fj.201700211R)
79. Ku DN, Giddens DP, Zarins CK, Glagov S. 1985 Pulsatile flow and atherosclerosis in the human carotid bifurcation. Positive correlation between plaque location and low oscillating shear stress. *Arteriosclerosis* **5**, 293–302. (doi:10.1161/01.ATV.5.3.293)
80. Gimbrone Jr MA, Garcia-Cardena G. 2013 Vascular endothelium, hemodynamics, and the pathobiology of atherosclerosis. *Cardiovasc. Pathol.* **22**, 9–15. (doi:10.1016/j.carpath.2012.06.006)
81. Truskey G, Yuan F, Katz D. 2009 *Transport phenomena in biological systems*. London, UK: Pearson Education Ltd.
82. Zarins CK, Giddens DP, Bharadvaj BK, Sottiurai VS, Mabon RF, Glagov S. 1983 Carotid bifurcation atherosclerosis. Quantitative correlation of plaque localization with flow velocity profiles and wall shear stress. *Circ. Res.* **53**, 502–514. (doi:10.1161/01.RES.53.4.502)
83. Tarbell JM, Shi Z-D, Dunn J, Jo H. 2014 Fluid mechanics, arterial disease, and gene expression. *Annu. Rev. Fluid Mech.* **46**, 591–614. (doi:10.1146/annurev-fluid-010313-141309)
84. Friedman MH, Deters O, Mark F, Brentbargeron C, Hutchins G. 1983 Arterial geometry affects hemodynamics: a potential risk factor for atherosclerosis. *Atherosclerosis* **46**, 225–231. (doi:10.1016/0021-9150(83)90113-2)
85. Liu X, Fan Y, Deng X, Zhan F. 2011 Effect of non-Newtonian and pulsatile blood flow on mass transport in the human aorta. *J. Biomech.* **44**, 1123–1131. (doi:10.1016/j.jbiomech.2011.01.024)
86. Olgac U, Kurtcuoglu V, Poulikakos D. 2008 Computational modeling of coupled blood-wall mass transport of LDL: effects of local wall shear stress. *Am. J. Physiol. Heart Circ. Physiol.* **294**, H909–H919. (doi:10.1152/ajpheart.01082.2007)
87. Iasiello M, Vafai K, Andreozzi A, Bianco N. 2016 Analysis of non-Newtonian effects on low-density lipoprotein accumulation in an artery. *J. Biomech.* **49**, 1437–1446. (doi:10.1016/j.jbiomech.2016.03.017)
88. Crawford DW, Back LH, Cole MA. 1980 *In vivo* oxygen transport in the normal rabbit femoral arterial wall. *J. Clin. Invest.* **65**, 1498–1508. (doi:10.1172/JCI109815)
89. Moore JA, Ethier CR. 1997 Oxygen mass transfer calculations in large arteries. *J. Biomech. Eng.* **119**, 469–475. (doi:10.1115/1.2798295)
90. Murphy EA, Dunne AS, Martin DM, Boyle FJ. 2016 Oxygen mass transport in stented coronary arteries. *Ann. Biomed. Eng.* **44**, 508–522. (doi:10.1007/s10439-015-1501-6)
91. Tarbell JM. 2003 Mass transport in arteries and the localization of atherosclerosis. *Annu. Rev. Biomed. Eng.* **5**, 79–118. (doi:10.1146/annurev.bioeng.5.040202.121529)
92. Fournier R. 2007 *Basic transport phenomena in biomedical engineering*, 2nd edn. London, UK: Taylor and Francis.
93. Tada S, Tarbell JM. 2006 Oxygen mass transport in a compliant carotid bifurcation model. *Ann. Biomed. Eng.* **34**, 1389–1399. (doi:10.1007/s10439-006-9155-z)
94. Qiu Y, Tarbell JM. 2000 Numerical simulation of pulsatile flow in a compliant curved tube model of a coronary artery. *J. Biomech. Eng.* **122**, 77–85. (doi:10.1115/1.429629)
95. Tsutsui H, Yamagishi M, Uematsu M, Suyama K, Nakatani S, Yasumura Y, Asanuma T, Miyatake K. 1998 Intravascular ultrasound evaluation of plaque distribution at curved coronary segments. *Am. J. Cardiol.* **81**, 977–981. (doi:10.1016/S0002-9149(98)00075-7)
96. Fernandez Esmerats J *et al.* 2019 Disturbed flow increases UBE2C (Ubiquitin E2 Ligase C) via loss of miR-483-3p, inducing aortic valve calcification by the pVHL (von Hippel–Lindau Protein) and HIF-1$\alpha$ (hypoxia-inducible factor-1$\alpha$) pathway in endothelial cells. *Arterioscler. Thromb. Vasc. Biol.* **39**, 467–481. (doi:10.1161/ATVBAHA.118.312233)
97. Lim CS, Gohel MS, Shepherd AC, Paleolog E, Davies AH. 2011 Venous hypoxia: a poorly studied etiological factor of varicose veins. *J. Vasc. Res.* **48**, 185–194. (doi:10.1159/000320624)
98. Lim CS, Davies AH. 2009 Pathogenesis of primary varicose veins. *Br. J. Surg.* **96**, 1231–1242. (doi:10.1002/bjs.6798)
99. Raffetto JD, Khalil RA. 2008 Mechanisms of varicose vein formation: valve dysfunction and wall dilation. *Phlebology* **23**, 85–98. (doi:10.1258/phleb.2007.007027)
100. Chiu JJ, Chien S. 2011 Effects of disturbed flow on vascular endothelium: pathophysiological basis and clinical perspectives. *Physiol. Rev.* **91**, 327–387. (doi:10.1152/physrev.00047.2009)
101. McCluskey RT, Wilens SL. 1953 The infrequency of lipid deposition in sclerotic veins. *Am. J. Pathol.* **29**, 71–83.
102. Lever MJ, Jay MT. 1990 Albumin and Cr-EDTA uptake by systemic arteries, veins, and pulmonary artery of rabbit. *Arteriosclerosis* **10**, 551–558. (doi:10.1161/01.ATV.10.4.551)
103. Meads C, Cummins MS, Jolly AC, Stevens E, Burls AH, Hyde M. 2000 Coronary artery stents in the treatment of ischaemic heart disease: a rapid and systematic review. *Health Technol. Assess.* **4**, 1–153. (doi:10.3310/hta4230)
104. Caro CG, Seneviratne A, Heraty KB, Monaco C, Burke MG, Krams R, Chang CC, Coppola G, Gilson P. 2013 Intimal hyperplasia following implantation of helical-centreline and straight-centreline stents in common carotid arteries in healthy pigs: influence of intraluminal flow. *J. R. Soc. Interface* **10**, 20130578. (doi:10.1098/rsif.2013.0578)
105. Cheema AN *et al.* 2006 Adventitial microvessel formation after coronary stenting and the effects of SU11218, a tyrosine kinase inhibitor. *J. Am. Coll. Cardiol.* **47**, 1067–1075. (doi:10.1016/j.jacc.2005.08.076)
106. Santilli SM, Tretinyak AS, Lee ES. 2000 Transarterial wall oxygen gradients at the deployment site of an intra-arterial stent in the rabbit. *Am. J. Physiol. Heart Circ. Physiol.* **279**, H1518–H1525. (doi:10.1152/ajpheart.2000.279.4.H1518)

107. Tretinyak AS, Lee ES, Uema KM, D'audiffret AC, Caldwell MP, Santilli SM. 2002 Supplemental oxygen reduces intimal hyperplasia after intraarterial stenting in the rabbit. *J. Vasc. Surg.* **35**, 982–987. (doi:10.1067/mva.2002.123090)
108. Gomes WJ, Buffolo E. 2006 Coronary stenting and inflammation: implications for further surgical and medical treatment. *Ann. Thorac. Surg.* **81**, 1918–1925. (doi:10.1016/j.athoracsur.2005.10.014)
109. Welt FG, Rogers C. 2002 Inflammation and restenosis in the stent era. *Arterioscler. Thromb. Vasc. Biol.* **22**, 1769–1776. (doi:10.1161/01.ATV.0000037100.44766.5B)
110. Yeh JS, Oh SJ, Hsueh CM. 2016 Frequency of vascular inflammation and impact on neointimal proliferation of drug eluting stents in porcine coronary arteries. *Acta Cardiol. Sin.* **32**, 570–577.
111. Caputo M, Chiastra C, Cianciolo C, Cutrã E, Dubini G, Gunn J, Keller B, Migliavacca F, Zunino P. 2013 Simulation of oxygen transfer in stented arteries and correlation with in-stent restenosis. *Int. J. Numer. Method Biomed. Eng.* **29**, 1373–1387. (doi:10.1002/cnm.2588)
112. Van der Heiden K, Gijsen FJH, Narracott A, Hsiao S, Halliday I, Gunn J, Wentzel JJ, Evans PC. 2013 The effects of stenting on shear stress: relevance to endothelial injury and repair. *Cardiovasc. Res.* **99**, 269–275. (doi:10.1093/cvr/cvt090)
113. Li Y, Hao Y, Wang T, Wei L, Wang W, Liang Y, Guo X. 2018 The effect of hyperbaric oxygen therapy on myocardial perfusion after the implantation of drug-eluting stents. *Ann. Clin. Lab. Sci.* **48**, 158–163.
114. Wan J, Lata C, Santilli A, Green D, Roy S, Santilli S. 2014 Supplemental oxygen reverses hypoxia-induced smooth muscle cell proliferation by modulating HIF-alpha and VEGF levels in a rabbit arteriovenous fistula model. *Ann. Vasc. Surg.* **28**, 725–736. (doi:10.1016/j.avsg.2013.10.007)
115. Sanada JI, Matsui O, Yoshikawa J, Matsuoka T. 1998 An experimental study of endovascular stenting with special reference to the effects on the aortic vasa vasorum. *Cardiovasc. Intervent. Radiol.* **21**, 45–49. (doi:10.1007/s002709900210)
116. Vasuri F, Fittipaldi S, Buzzi M, Degiovanni A, Stella A, D'Errico-Grigioni A, Pasquinelli G. 2012 Nestin and WT1 expression in small-sized vasa vasorum from human normal arteries. *Histol. Histopathol.* **27**, 1195–1202.
117. Kantor B, Mohlenkamp S. 2003 Imaging of myocardial microvasculature using fast computed tomography and three-dimensional microscopic computed tomography. *Cardiol. Clin.* **21**, 587–605, ix. (doi:10.1016/S0733-8651(03)00110-3)
118. Zahedmanesh H, Lally C. 2009 Determination of the influence of stent strut thickness using the finite element method: implications for vascular injury and in-stent restenosis. *Med. Biol. Eng. Comput.* **47**, 385–393. (doi:10.1007/s11517-009-0432-5)
119. Karimi A, Navidbakhsh M, Razaghi R. 2014 A finite element study of balloon expandable stent for plaque and arterial wall vulnerability assessment. *J. Appl. Phys.* **116**, 044701. (doi:10.1063/1.4891019)
120. Schiavone A, Zhao LG, Abdel-Wahab AA. 2014 Effects of material, coating, design and plaque composition on stent deployment inside a stenotic artery—finite element simulation. *Mater. Sci. Eng. C Mater. Biol. Appl.* **42**, 479–488. (doi:10.1016/j.msec.2014.05.057)
121. Corti A, DePaolis A, Tarbell J, Cardoso L. 2019 Evaluation of stenting induced vasa vasorum compression. In *Proc. of the 25th Congr. of the European Society of Biomechanics, 7–10 July, Vienna, Austria*, p. 119. See https://owncloud.tuwien.ac.at/index.php/s/dovqqcj02VeZHze.
122. Im E, Hong MK. 2016 Drug-eluting stents to prevent stent thrombosis and restenosis. *Expert Rev. Cardiovasc. Ther.* **14**, 87–104. (doi:10.1586/14779072.2016.1112267)
123. Lee SY, Bae I-H, Sung Park D, Jang E-J, Shim J-W, Lim K-S, Park J-K, Sim DS, Jeong MH. 2016 Prednisolone- and sirolimus-eluting stent: anti-inflammatory approach for inhibiting in-stent restenosis. *J. Biomater. Appl.* **31**, 36–44. (doi:10.1177/0885328216630498)
124. Shinke T *et al.* 2008 Abstract 6059: Novel helical stent design elicits swirling blood flow pattern and inhibits neointima formation in porcine carotid arteries. *Circulation* **118**(Suppl. 18), S1054.
125. Coppola G, Caro C. 2009 Arterial geometry, flow pattern, wall shear and mass transport: potential physiological significance. *J. R. Soc. Interface* **6**, 519–528. (doi:10.1098/rsif.2008.0417)
126. Coppola G, Caro C. 2008 Oxygen mass transfer in a model three-dimensional artery. *J. R. Soc. Interface* **5**, 1067–1075. (doi:10.1098/rsif.2007.1338)
127. Zeller T, Gaines PA, Ansel GM, Caro CG. 2016 Helical centerline stent improves patency: two-year results from the randomized mimics trial. *Circ. Cardiovasc. Interv.* **9**, e002930. (doi:10.1161/CIRCINTERVENTIONS.115.002930)
128. De Nisco G, Kok AM, Chiastra C, Gallo D, Hoogendoorn A, Migliavacca F, Wentzel JJ, Morbiducci U. 2019 The atheroprotective nature of helical flow in coronary arteries. *Ann. Biomed. Eng.* **47**, 425–438. (doi:10.1007/s10439-018-02169-x)
129. Kohler TR, Jawien A. 1992 Flow affects development of intimal hyperplasia after arterial injury in rats. *Arterioscler. Thromb.* **12**, 963–971. (doi:10.1161/01.ATV.12.8.963)
130. Kohler TR, Kirkman TR, Kraiss LW, Zierler BK, Clowes AW. 1991 Increased blood flow inhibits neointimal hyperplasia in endothelialized vascular grafts. *Circ. Res.* **69**, 1557–1565. (doi:10.1161/01.RES.69.6.1557)
131. Garanich JS, Pahakis M, Tarbell JM. 2005 Shear stress inhibits smooth muscle cell migration via nitric oxide-mediated downregulation of matrix metalloproteinase-2 activity. *Am. J. Physiol. Heart Circ. Physiol.* **288**, H2244–H2252. (doi:10.1152/ajpheart.00428.2003)